Title

Safety profile after prolonged C3 inhibition.

Authors

Reis, Edimara S
Berger, Nadja
Wang, Xin
et al.

Publication Date

2018-12-01

DOI

10.1016/j.clim.2018.09.004

Peer reviewed

HHS Public Access

Author manuscript

Clin Immunol. Author manuscript; available in PMC 2019 December 01.

Published in final edited form as:

Clin Immunol. 2018 December ; 197: 96–106. doi:10.1016/j.clim.2018.09.004.

Safety Profile After Prolonged C3 Inhibition

Edimara S. Reis[1], **Nadja Berger**[1], **Xin Wang**[1], **Sophia Koutsogiannaki**[1], **Robert K. Doot**[2], **Justin T. Gumas**[1], **Periklis G. Foukas**[3], **Ranillo R.G. Resuello**[4], **Joel V. Tuplano**[4], **David Kukis**[5], **Alice F. Tarantal**[6], **Anthony J. Young**[2], **Tetsushiro Kajikawa**[7], **Athena Soulika**[8], **Dimitrios C. Mastellos**[9], **Despina Yancopoulou**[10], **Ali-Reza Biglarnia**[11], **Markus Huber-Lang**[12], **George Hajishengallis**[7], **Bo Nilsson**[13], and **John D. Lambris, PhD**[1]

[1]Department of Pathology and Laboratory Medicine, Perelman School of Medicine, University of Pennsylvania, Philadelphia PA 19104, USA

[2]Department of Radiology, Perelman School of Medicine, University of Pennsylvania, Philadelphia PA 19104, USA

[3]2nd Department of Pathology, National and Kapodistrian University of Athens, Attikon University Hospital, Athens, Greece

[4]Simian Conservation Breeding and Research Center (SICONBREC), Makati City, Philippines

[5]Center for Molecular and Genomic Imaging, University of California, Davis, CA 95616, USA

[6]Departments of Pediatrics and Cell Biology and Human Anatomy, School of Medicine, and California National Primate Research Center, University of California, Davis, CA 95616, USA

[7]Department of Microbiology, School of Dental Medicine, University of Pennsylvania, Philadelphia, PA 19104, USA

[8]Department of Dermatology, University of California, Davis, CA 95616, USA

[9]National Center for Scientific Research ‘Demokritos’, Athens, Greece

[10]Amyndas Pharmaceuticals, Glyfada, Greece

[11]Department of Transplantation, Skane University Hospital, Lund University, Lund, Sweden

[12]Institute of Clinical and Experimental Trauma-Immunology, University Hospital Ulm, Ulm, Germany

[13]Department of Immunology, Genetics and Pathology, Uppsala University, Uppsala, Sweden

Abstract

Correspondence: John D. Lambris, PhD, University of Pennsylvania, School of Medicine, Department of Pathology and Laboratory Medicine, 401 Stellar Chance Labs, 422 Curie Blvd., Philadelphia, PA 19104-6100, lambris@pennmedicine.upenn.edu.

The other authors declare no competing interests.

The central component of the complement cascade, C3, is involved in various biological functions, including opsonization of foreign bodies, clearance of waste material, activation of immune cells, and triggering of pathways controlling development. Given its broad role in immune responses, particularly in phagocytosis and the clearance of microbes, a deficiency in complement C3 in humans is often associated with multiple bacterial infections. Interestingly, an increased susceptibility to infections appears to occur mainly in the first two years of life and then wanes throughout adulthood. In view of the well-established connection between C3 deficiency and infections, therapeutic inhibition of complement at the level of C3 is often considered with caution or disregarded. We therefore set out to investigate the immune and biochemical profile of non-human primates under prolonged treatment with the C3 inhibitor compstatin (Cp40 analog). Cynomolgus monkeys were dosed subcutaneously with Cp40, resulting in systemic inhibition of C3, for 1 week, 2 weeks, or 3 months. Plasma concentrations of both C3 and Cp40 were measured periodically and complete saturation of plasma C3 was confirmed. No differences in hematological, biochemical, or immunological parameters were identified in the blood or tissues of animals treated with Cp40 when compared to those injected with vehicle alone. Further, skin wounds showed no signs of infection in those treated with Cp40. In fact, Cp40 treatment was associated with a trend toward accelerated wound healing when compared with the control group. In addition, a biodistribution study in a rhesus monkey indicated that the distribution of Cp40 in the body is associated with the presence of C3, concentrating in organs that accumulate blood and produce C3. Overall, our data suggest that systemic C3 inhibition in healthy adult non-human primates is not associated with a weakened immune system or susceptibility to infections.

Keywords

complement; C3; compstatin; Cp40; AMY-101; inflammation; infection; non-human primate

1. Introduction

The complement system is perceived as a first line of defense against microbes and foreign matter [1, 2]. Complement component C3, in particular, has a central role in the activation and amplification of the complement cascade, and biologically active fragments generated during its activation play an integral role in body surveillance and modulation of immune responses [3]. Whereas the C3a and C3dg activation fragments can trigger cell activation upon binding to their respective receptors, C3aR and complement receptor 2 (CR2), the fragments C3b and iC3b ensure proper opsonization and clearance of immune complexes, damaged cells, debris, and pathogens [3, 4]. Since complement functionality is entirely contingent on C3, disruption of C3 protein as a result of gene mutations or the presence of auto-antibodies is often associated with pathological conditions [4, 5]. Indeed, patients deficient in C3 as a consequence of genetic mutations often suffer from multiple infections and have an increased susceptibility to autoimmune and kidney disease. Notably, symptoms have an early onset (~2 years of age) and appear to become less severe during adulthood, when the immune system is fully developed [3, 6].

Although insufficient levels of C3 are undesirable for a healthy organism, excessive generation of C3 activation products resulting from a dysregulation of the complement

cascade is even more troublesome. Genetic variants of C3 or other complement proteins such as Factor B (FB), FH, and FI, with modified binding properties, disrupt the functioning of the cascade and often result in deregulated complement activation. As a consequence, maladaptive activation of immune cells fuels inflammatory responses that lead to tissue damage and pathology [7, 8]. Indeed, increased levels of complement activation products are observed in a variety of conditions, including hematological, neurological, renal, and cardiovascular diseases, as well as obesity, asthma, cancer, periodontitis, and transplant rejection [9–17].

In light of the abovementioned information and given the central role of C3 in complement activation, amplification, and effector function, therapeutic intervention to inhibit C3 activation appears to be a promising option to modulate the maladaptive inflammation observed in complement-mediated disorders [18–20]. In line with this idea, peptidic compounds, particularly derivatives of compstatin that specifically bind C3 from human and non-human primates and inhibit C3 activation, are currently under clinical development [21, 22]. Some compstatin analogs, i.e., APL-2 (Apellis Pharmaceuticals), and AMY-101 (Amyndas Pharmaceuticals), are being clinically developed for the treatment of paroxysmal nocturnal hemoglobinuria (PNH), age-related macular degeneration (AMD), C3 glomerulopathies, cold agglutinin disease, and other complement-mediated conditions. APL-2 has already shown positive results in PNH and AMD clinical trials and both APL-2 and AMY-101 have shown a good safety profile without any concerns [20].

Despite these promising clinical results, systemic inhibition of C3 is still considered with caution. Although pre-clinical and clinical studies in non-human primates and humans, respectively have identified suitable routes for drug administration and established the feasibility of inhibiting C3 despite its high protein concentration in the plasma (~1 mg/mL) [22, 23], safety concerns, including the possibility of increased susceptibility to infections, autoimmune and kidney disease, are still a cause of skepticism regarding C3-targeted inhibition. As compstatin analogs are not active in rodents, rabbits, pigs, dogs, or other experimental animals [21], safety studies in non-human primates are required. Therefore, we investigated the clinical, hematologic, and biochemical profile of cynomolgus monkeys under treatment with compstatin (Cp40 analog [22, 24]) for up to 3 months. After the treatment period, full necropsy, complete histopathologic examination, and evaluation of cytokine expression were conducted in animals from both the treatment (Cp40) and control (vehicle) groups. In addition, we also conducted a positron emission tomography/ computed tomography (PET/CT) imaging study in order to address biodistribution in a rhesus monkey which indicated that the distribution of Cp40 in the body is associated with the presence of C3, concentrating in organs that accumulate blood and produce C3. Here, for the first time, we show data supporting the safety of C3 inhibition therapy and the absence of any signs of infection, inflammation, auto-immune disease or tissue damage in adult monkeys treated with Cp40.

Material and methods

1.1. C3 inhibitor Cp40

Cp40 (dTyr-Ile-[Cys-Val-Trp(Me)-Gln-Asp-Trp-Sar-Ala-His-Arg-Cys]-mIle-NH_2, 1.8 kDa) was produced by solid-phase peptide synthesis as previously described [24]. Peptides were purified by reversed-phase high-performance liquid chromatography, characterized by mass spectrometry [24], and tested for the presence of endotoxin (< 0.03 EU/mL).

1.2. Injection of Cp40 into cynomolgus monkeys

A total of 33 cynomolgus monkeys (*Macaca fascicularis*) housed at the Simian Conservation Breeding and Research Center (SICONBREC, Makati City, Philippines) were used in this study. Monkeys (25 males and 8 females) were ~5 years of age, weighed ~4 kg, and were considered healthy after evaluation by an experienced veterinarian. Prior to the study, the animals were acclimatized for 2 weeks in the experimental room under conditions of controlled temperature (26 ± 4 °C), relative humidity (60 ± 25 %), and ventilation and a natural day and night cycle. Animals were provided with 100 g of food (standard monkey grower pellets, Jetstar Milling Corporation, Lipa Batangas, Philippines) daily and with water *ad libitum* (via water bottle) throughout the acclimation and observation periods. A fresh banana was given daily as supplementary diet. On the day of dosing, food was provided after the administration of the compound. Adult animals were injected subcutaneously or intravenously every 24 or 48 h with 2, 3, 4, or 20 mg/kg of Cp40 dissolved in sterile saline or water for injection containing 5% dextrose. Blood samples (1–2 ml) were collected from the femoral vein into EDTA-vacutainer tubes immediately before and at various time points after compound injection. Samples were centrifuged at 800 × *g* for 10 min to obtain plasma and immediately frozen at ≤ −80 °C until further analysis.

Full hematologic and biochemical evaluations, using a Mythic 18 VET- hematology analyzer and Microlab 300 semi-automated clinical chemistry analyzer, were also conducted on blood and serum samples collected from all animals in the study. The parameters measured were: white blood cell count, red blood cell count, hemoglobin, hematocrit, mean corpuscular volume, mean corpuscular hemoglobin, mean corpuscular hemoglobin concentration, red cell distribution width, platelet count, thrombocrit, mean platelet volume, platelet distribution width, lymphocyte count, monocyte count, granulocyte count, prothrombin time, activated partial thromboplastin time, reticulocyte count, glucose, total cholesterol, triglycerides, blood urea nitrogen, creatinine, total protein, albumin, globulin, total bilirubin, amylase, glutamate oxaloacetate transaminase, glutamate pyruvic transaminase, alkaline phosphatase, gamma glutamyl transferase, magnesium, calcium, inorganic phosphorous, chloride, potassium, and sodium. The values obtained were compared with normal reference values previously obtained in cynomolgus monkeys [25].

Animals were sedated using ketamine (5–10 mg/kg) and xylazine (1–2 mg/kg) before blood collection. Atropine sulphate (0.04 mg/kg) was given prior to anesthesia. Where indicated, animals were euthanized, and full necropsy with histologic assessment was performed. All cynomolgus monkeys studies were performed in accordance with animal welfare laws and regulations, as approved by the Institutional Animal Care and Use Committee (IACUC).

SICONBREC is accredited by the Association for Assessment and Accreditation of Laboratory Animal Care (AAALAC).

1.3. Quantitation of Cp40 and C3 in the plasma

Levels of Cp40 in the plasma of cynomolgus monkeys were determined after methanol precipitation of Cp40 from plasma samples and quantification by reversed-phase liquid chromatography coupled with mass spectrometry, with a detection limit of 0.18 μg/ml (100 nM) [22]. The plasma concentration of C3 was determined using nephelometry as previously described [26].

1.4. Wound healing model

A model of wound healing was established in cynomolgus monkeys. Animals were anesthetized by an intramuscular injection of ketamine (10–12 mg/kg) plus xylazine (2 mg/kg) on the day of surgery. The skin on the back was cleaned, shaved, and sterilized with betadine followed by 4% chlorhexidine and 70% isopropyl alcohol. Four excisional punch biopsies (8- mm diameter and full skin thickness) were taken from the back of each animal. The borders of the wounds were marked using indelible, nontoxic ink and each site was covered with a sterile gauze dressing with Chlorhexidine (0.40% to 0.60%) for 2 h after surgery. The animals were then placed in a jacket (Lomir Biomedical, Inc., Quebec, Canada) that does not restrict mobility but prevents them from scratching the biopsy site and housed individually to prevent any potential wound disturbance by other animals. Ketorolac (0.5 mg/kg) was given twice a day to prevent pain.

Animals in the treatment group received the compstatin analog Cp40 (2 mg/kg subcutaneously, every 12 h for 7 days; n=4), and control animals were injected with vehicle (water plus 5% dextrose, same injection scheme; n=4). The size of each biopsy site was monitored daily until complete healing occurred and digitally documented. ImageJ2 software (National Institutes of Health) was used to calculate changes in wound area over time. Repair of the wound area was calculated as the percentage of area of the original wound.

Additional skin biopsies (12 mm) were collected at days 5 and 12 from the healing wounds; tissues were snap-frozen in liquid N_2 and stored at ≤ −80 °C until further use. These sections of skin biopsies were fixed in 10% formalin for hematoxylin and eosin (H&E) staining. The fixed tissues were dehydrated in graded concentrations of alcohol, cleared in xylene, and infiltrated and embedded in paraffin. Paraffin blocks for each animal were then sectioned at 5-μm thickness and stained with H&E for gross histologic examination. H&E slides were scanned with a D.SIGHT 200 fluo slide scanner (Menarini Diagnostic, Italy), and images of the sections were acquired at 2× magnification.

1.5. Measurement of residual complement activity in the plasma

The residual complement activity was assessed in plasma samples of cynomolgus monkeys from both Cp40-treatment and control groups using a standard hemolytic assay. Briefly, rabbit blood cells (5% v/v) were incubated with 10% plasma in GVB-Mg^{2+} buffer (150 μl total volume) for 1 h at 37 °C in a 96-well plate. The plate was spun down and 100 μl of

supernatant was transferred to clean wells. Absorbance was measured at 405 nm and converted into % of activation, where 100% activation equals to the O.D. obtained in plasma samples collected at time point 0 h, previous to treatment initiation. The relative residual complement activity measured in plasma samples containing Cp40 was plotted against the peptide concentration using GraphPad Prism 5 (La Jolla, CA).

1.6. Quantitative Real-Time RT-PCR

RNA was extracted from skin punch biopsies or tissue specimens collected during necropsy of cynomolgus monkeys by using the RNeasy® Fibrous Tissue Mini (Qiagen, Germantown, MD) or RNeasy® Mini (Qiagen) kits, respectively. RNA concentration and purity were assessed using a NanoDropTM 2000c spectrophotometer (Thermo Fisher Scientific). Samples with an A_{260}/A_{280} ratio of ~2.0 and A_{260}/A_{230} ratio ≥1.8 were reverse-transcribed by using a High-Capacity cDNA Reverse Transcription kit (Applied Biosystems, Foster City, CA). The resulting cDNA was further amplified using TaqMan® Fast Universal PCR Master Mix (Applied Biosystems) on a StepOnePlus Real-Time PCR System (Applied Biosystems) according to the manufacturer's instructions. Custom TaqMan® Array 96 - Well FAST Plates (Applied Biosystems) were designed containing the following *Macaca fascicularis*-specific probes: Mf02789775_m1 (*IL1B*), Mf02789780_m1 (*IL2*), Mf00541746_m1 (*IL4I1*), Mf02789322_m1 (*IL6*), Mf02789706_g1 (*IL8*), Mf02789325_m1 (*IL10*), Mf02789753_m1 (*IL12B*), Mf03043053_m1 (*IL13*), Mf04367377_m1 (*IL17A*), Mf02877343_m1 (*IL22*), Mf02794722_m1 (*C3*), Mf04385270_g1 (*CXCL5*), Mf02787883_m1 (*FGF2*), Mf02788577_m1 (*IFNG*), Mf00966524_m1 (*PDGFB*), Mf04389740_m1 (*SELE*), Mf04384675_m1 (*SELP*), Mf00998133_m1 (*TGFB1*), Mf02789784_g1 (*TNF*), Mf04383655_g1 (*VEGFB*). Expression of target mRNA was normalized using the signal obtained from the amplification with the 18S probe (Hs99999901_s1).

1.7. Cp40 iodination- Rhesus monkey imaging study

In order to study the biodistribution of Cp40 in PET imaging studies, Cp40 was labeled with the [^{124}I] tracer. [^{124}I]KI (IBA; 3.75 mCi) in 20 mM NaOH was buffered with 100 mM HCl and 1 M HEPES, pH 7. The following were then added: carrier KI (VWR; 0.67 μmol), Cp40 (0.67 μmol) in 0.3% Tween-20, and Chloramine-T (0.67 μmol) in a total volume of 563 μl. Cp40 precipitated immediately when the Chloramine-T was added but returned to solution with the addition of 10% Tween-20 (70 μl) to the reaction. The reaction was allowed to proceed for 3.5 min at room temperature and then quenched by adding 30 mM sodium metabisulfite (1.0 μmol). The quenched reaction was immediately diluted in water (15 ml) and loaded onto a Sep Pak C18 light SPE cartridge. The cartridge was washed in water (3 ml), then peptide (1.9 mCi) was eluted in ethanol (1.5 ml). HPLC evaluation of the SPE eluent indicated recovery of 43% of the total radioactivity as [^{124}I]Cp40, i.e., 0.82 mCi; thus, the radiochemical yield was 0.82 mCi/3.75 mCi = 22%.

The SPE eluent was then reduced in volume to near dryness under a gentle stream of helium at room temperature. The dose was formulated without further purification of [^{124}I]Cp40. Cold Cp40 was added to achieve the desired formulation of 1.0 mCi [^{124}I] / 5.0 mg total Cp40/ 1.4 ml for the 2.55 kg animal, plus excess for transfer loss; the dose was syringe end-

filtered (0.22 μm) into a sterile vial. HPLC evaluation of the final dose indicated 45% of total radioactivity as [^{124}I]Cp40.

1.8. Injection of [^{124}I]Cp40 and PET imaging

A female juvenile rhesus monkey, ~1.5 years of age (2.55 kg), was sedated with telazol (intramuscular; 5–8 mg/kg) and injected subcutaneously with 41.85 MBq (1.131 mCi) [^{124}I]Cp40 (0.20 mCi/mg specific activity; 5.66 Cp40 mass [mg]; ~1 ml). Blood samples (~2 ml, peripheral vessel) were collected into EDTA at −1 min, then at 0, +5, and +30 min and at 1, 4, 8, 24, 48, 72, and 240 h post-injection and counted to enable calculation of the percentage of the injected dose (%ID) per mL of plasma. PET/CT imaging (GE Discovery® PET/CT) was performed post-injection under telazol sedation: after 30 min (20-min duration of scan), after 4 h (20-min duration of scan) and after 1, 2, 3, and 10 days (40-min duration scan on each day). The animal was placed on the scan bed according to standard operating procedures and maintained in a radioactive monitoring housing area to address radioactive waste for the duration of the study.

Representative fused PET/CT images projections (MIP) from the scans acquired 1, 3, and 10 days after injection of [$_{124}$I]Cp40 were captured using MIM version 6.7 (MIM Software Inc., Cleveland, OH). The total activities residing in regions of high radiotracer concentration including the injection site, thyroids, gallbladder, liver, intestines, spleen, heart, and urinary bladder for each time point were determined from volumes of interest measurements of the PET images using Pmod v3.7 image analysis software package (PMOD Technologies Ltd., Zurich, Switzerland). The resulting regional total activities were decay-corrected and divided by the injected dose to yield percentages of injected doses for each time point. Regional %IDs were subsequently plotted as functions of time using GraphPad Prism 7 (La Jolla, CA).

This study was conducted at the UC Davis California National Primate Research Center. All animal procedures conformed to the requirements of the Animal Welfare Act and protocols were approved prior to implementation by the UC Davis IACUC. UC Davis is an AAALAC-accredited institution.

2. Results

2.1. In vivo distribution of Cp40 is associated with the presence of C3

The pharmacokinetic profile of the C3 inhibitor Cp40 has been extensively investigated and shows a plasma half-life of ~40 h after a single subcutaneous dose of 2 mg/kg. The peptide reaches maximum concentration in the plasma at 2 h post-injection, followed by a slow elimination phase and resulting in complete C3 saturation for ~4.5 h [22, 24]. To further understand the biodistribution of Cp40, a rhesus monkey was dosed subcutaneously with 42 MBq of [^{124}I]-labeled Cp40 (2.2 mg/kg of Cp40), followed by PET/CT scans performed over time to measure changing radioactivity concentrations in the organs. Fused PET/CT images of the *in vivo* distribution of [^{124}I]Cp40 are displayed in Fig. 1A, B and percentages of injected doses in the regions with the highest concentrations of [^{124}I]-labeled Cp40 are shown as a function of time (Fig. 1C). The highest percentage of the injected dose was

located at the subcutaneous injection site (Fig. 1A), indicating the presence of a depot compartment exhibiting a delayed release of radiotracer into the circulation, with percentages of injected dose remaining at the injection site steadily decreasing from 64 %ID after 30 minutes to 19 %ID after 10 days. Highest regional uptakes of [^{124}I]Cp40 based on the areas under the curve (AUC) for percentages of the injected dose over time in descending order were; the injection site, thyroid, gallbladder, liver, intestines, spleen, heart, and urinary bladder (7683, 152, 110, 87, 46, 31, 21, and 11 %•hr) (Fig. 1C). The fourth highest regional amount of [^{124}I]Cp40 by AUC was detected in the liver (Fig. 1C), the main source of C3 in the body [27]. High levels of [^{124}I]Cp40 in the gallbladder and intestines may be due to hepatobiliary excretion of the PET radiotracer (Fig. 1). The radioactivity in the heart may primarily reflect the presence of [^{124}I]Cp40 in the blood since the highest uptakes in the heart of 0.34 %ID and in blood plasma of 0.05%ID/mL both peaked at 4 hours post-injection (Fig. 1). Ten days after injection of [^{124}I]Cp40, radiotracer uptake was primarily observed in the injection site, thyroids, and gallbladder (Fig. 1). In general, radiotracer concentrations decreased over time everywhere except for the thyroid, which exhibited increasing concentrations that may be due to the iodine radiotracer attached to Cp40 [28] (Fig. 1). Nasal accumulation of [^{124}I]Cp40 was faintly visible in the sagittal PET/CT image acquired 1 day post-injection (Fig. 1A) and is a typical finding for compounds labeled with iodine [29]. Overall these data, with the exception of high thyroid uptake of [^{124}I]Cp40 likely due to the iodine radiolabel, indicate that the body distribution of Cp40 is associated with the presence of C3, concentrating in organs that accumulate blood (heart, spleen, liver) and produce C3 (liver, spleen).

2.2. In vivo C3 inhibition during a one-week period

We next investigated whether systemic blockage of C3 for a period of 7 days would affect immune and biochemical parameters measured in the blood of cynomolgus monkeys. To this end, monkeys were dosed subcutaneously with 2 mg/kg of Cp40 every 12 h for a total of 7 days; control animals were injected with vehicle (water plus 5% dextrose) according to the same schedule (Fig. 2A). During the 7-day period, the plasma concentrations of C3 remained constant in both the control and Cp40-treatment groups (Fig. 2B). Also, the Cp40 dosing schedule ensured constant levels of peptide that exceeded the concentration of C3, indicating complete saturation of plasma C3 by the Cp40 inhibitor (Fig. 2B, right panel). Complete inhibition of C3 over the 7-day period was confirmed by the absence of residual complement activity in the plasma of the animals treated with Cp40, whereas plasma samples from control animals retained full ability to activate complement (Fig. 2C).

Given that systemic inhibition of C3 was achieved for a period of 1 week, we then profiled immunologic, coagulation and biochemical parameters in the blood of monkeys at day 7 post-treatment and compared with the baseline values obtained prior to Cp40 injection (day 0) (Fig. 2D). Despite the C3 inhibition, no differences in hematological, coagulation and biochemical parameters were identified in the blood of animals treated with Cp40 when compared with those injected with vehicle alone (data not shown). Furthermore, blood cell counts, including counts of total white blood cells, red blood cells, platelets, and monocytes, were within the normal range and were not influenced by the Cp40 treatment (Fig. 2D). Although both control and treatment groups showed an elevated granulocyte count and

decreased lymphocyte count at day 7 when compared with baseline values, the values remained within the normal range observed in healthy animals (Fig. 2D).

In parallel, at 3 h after the initial injection of Cp40, the local immune response was triggered in these animals by skin biopsies. A total of four punch biopsies were taken from the dorsal side of each animal, and the size of each site was monitored daily until complete healing had occurred (Fig. 3A). Notably, the wounds showed no signs of infection (no antibiotics administered). In line with these observations, mRNA expression levels of cytokines (IL-2, IL-6, IL-8, IL-10, IL-13, IL-17, IL-22, CXCL5, TNF, TGF-β) and other molecules associated with wound healing (SELP, PDGFB, FGF2, SELE, LEGFB) were similar in skin biopsies from the control and treated animals, indicating an absence of local active infection despite Cp40 treatment (data not shown). Gross histologic observation showed no appreciable differences between the wounds biopsied from control and Cp40-treated animals (Fig. 3B). Skin biopsies showed sites of necrosis and ulceration, vascular and fibroblastic proliferation, and infiltration of inflammatory cells in the dermis at day 5 post-biopsy and an inflammatory exudate, scarring of the dermis, and reconstruction of the epidermis at day 12 post-biopsy (Fig. 3B), illustrating the classic inflammatory and proliferative phases of wound healing [30]. Further, C3 inhibition did not result in delayed healing. Instead, Cp40 treatment was associated with a trend toward faster wound healing than in control animals (Fig. 3C), suggesting that the therapeutic inhibition of C3 may modulate the local wound environment and promote the healing process.

2.3. In vivo C3 inhibition during a 2-week period

Cp40 treatment and consequent C3 inhibition was then extended for 2 weeks. During this extended treatment, systemic toxicity was also evaluated in response to the administration of a dose 10-fold higher than the established therapeutic dose (2–4 mg/kg). Cynomolgus monkeys were therefore dosed daily with intravenous infusions of 20 mg/kg of Cp40 for a total of 14 days, whereas control animals were injected with vehicle alone (Fig. 4A). The Cp40 dosing schedule resulted in a discrete accumulation of peptide in the circulation (from ~6 μM at day 0 to ~8 μM at day 12) and ensured the saturation of C3 in the plasma over the course of the entire treatment (Fig. 4B). After the last injection, on day 14, levels of plasma Cp40 rapidly decreased and were completely cleared by day 24 (Fig. 4B).

The animals were observed for a total of 40 days, and no mortality, clinical signs, effects on body weight and food consumption, or changes in clinical parameters such as body temperature, heart and respiratory rate, urine output, or blood pressure were observed in the animals treated with Cp40 (data not shown), indicating that the compound is well tolerated and does not induce systemic toxicity following repeated intravenous administration. Similarly, hematological (Fig. 4C), coagulation and blood chemistry (data not shown) clinical tests did not detect any changes directly induced by the peptide. Upon scheduled endpoint, histopathologic examination of the lung showed isolated areas of hemosiderosis (4 of 6 animals), atelectasis (1 of 6 animals) and anthracosis (2 of 6 animals). Signs of hemosiderosis and moderate to severe pulmonary edema were also found in animals from the control group that had been treated with vehicle alone, indicating that these observations

are unrelated to the treatment (Supplementary Table 1). With the exception of the lungs, all other organs were unremarkable with no adverse finding (Supplementary Table 1).

Expression levels of C3 mRNA in the spleen and liver of animals treated with Cp40 were similar to the levels found in tissues from those in the control group (Figure 4D, left panel). Similarly, no changes were observed in the mRNA expression of the proinflammatory cytokines IL-1β, IL-6, IL-10, IL-12, or IFN-γ in the spleen of Cp40-treated animals when compared with control spleens (Figure 4D, right panel), confirming that none of the treated animals showed any signs of infection or autoimmune disease during the trial period or during the 28 days following the administration of the peptide. Interestingly, an increase in the mRNA expression levels of the IL-22 cytokine was observed in the spleens of the Cp40-treated animals when compared with the expression of the same cytokine in the control group (Figure 4D, right panel).

2.3. In vivo C3 inhibition during a 3-month period

Next, systemic toxicity and treatment-associated effects were evaluated during a 3-month period in which cynomolgus monkeys were injected daily with 3 mg/kg of Cp40 subcutaneously (Fig. 5A); animals in the control group were injected with vehicle alone. Again, saturation of C3 concentrations in the plasma was observed during the entire treatment period (Fig. 5B).

No mortality, clinical signs, effects on body weight and food consumption, or changes in clinical parameters such as body temperature, heart and respiratory rate, urine output, or blood pressure were observed in the animals treated with Cp40 (data not shown), indicating that the compound is well tolerated and does not induce systemic toxicity following long-term administration. Similarly, hematological (Fig. 5C), coagulation and blood chemistry (data not shown) clinical tests did not detect any changes directly induced by the peptide. Upon necropsy, histopathologic examination of the subcutaneous tissue showed local inflammatory infiltrate in 6 of 8 animals in the treatment group (Supplementary Table 2), likely a consequence of the repeated subcutaneous injections with peptide. Animals from both the treatment and control groups showed lung atelectasis (Supplementary Table 2), a consequence of lung collapse during opening of the chest cavity. Apart from the subcutaneous tissue, no other organ indicated any adverse findings (Supplementary Table 2).

3. Discussion

In the present study, we show evidence of a safe outcome in response to systemic inhibition of complement C3 in non-human primates. Therapeutic inhibition of C3 in cynomolgus monkeys for up to 3 months using the compstatin analog Cp40 was not associated with any clinical signs or changes in hematologic, coagulation, or biochemical profiles. These findings therefore offer novel insight into the long-standing concern as to whether systemic inhibition of C3 would be associated with increased susceptibility to infections, autoimmune and/or kidney disease [31]. In addition, the precise assessment of drug biodistribution, exposure, and clearance and comprehensive histopathologic evaluation offer fundamental information to guide further development of therapeutic agents that target complement proteins.

Therapeutic inhibition of C3 has long been speculated to be a challenging and demanding approach to avoiding undesired effects of complement activation; therefore, it has been neglected, with researchers instead preferring strategies targeting proteins that, unlike C3, are not central to all three pathways of complement activation [20, 32]. The development of an antibody that blocks C5 activation has certainly been a hallmark in the field of complement therapeutics, alleviating clinical signs in patients suffering from complement-mediated diseases such as PNH and atypical hemolytic uremic syndrome (aHUS) [33, 34]. Anti-C5 therapy, however, has limitations, such as the presence of C3-mediated extravascular hemolysis in PNH patients and inefficacy in patients carrying certain mutations in the *C5* gene [35, 36]. The development of a safe approach to target C3 is therefore of clinical interest, filling a void in alternative treatments and possibly offering advantages over anti-C5 therapy under conditions in which the presence of excessive levels of C3 activation products contributes to the severity of the disease [18–20].

Previous pre-clinical studies using compstatin analogs have established the feasibility of saturating systemic C3, despite the high concentration of this protein in the plasma [9, 22, 24, 37]. Our data support the likelihood of complete C3 inhibition using Cp40 doses of ~2–4 mg/kg. Notably, when therapy discontinuation proves necessary, Cp40 is completely cleared from the body in ~6 days, avoiding any undesirable therapy-related adverse reaction. Further, the whole body serial PET scans indicate that the compound is distributed in the body dependent on the C3 localization or elimination; i.e., gallbladder, liver, intestines, spleen, heart and urinary bladder (with the noted exception of the high uptake of [^{124}I]Cp40 in thyroids that is likely due to the iodine [^{124}I] radiotracer). The urinary bladder is not a typical source of C3, except in cases of proteinuria associated with kidney disease [38]. However, this biodistribution study indicates a combination of hepatobiliary and renal clearance as routes of [^{124}I]Cp40 elimination. It is noteworthy that the biodistribution study was performed in a healthy juvenile rhesus monkey, where complement activation is expected to be under regulation. One can speculate that under conditions of disease with excessive complement activation, the biodistribution of the compound will vary dependent on the type of disease, level of complement activation, and affected organ. In line with this notion, although no radioactivity was observed in the brain, neurological conditions such as stroke where the blood-brain barrier is disrupted could benefit from Cp40 treatment, as Cp40 may be transported to the sites of inflammation in the brain [39, 40].

Complement has previously been implicated in the process of wound healing [41–43]. It is noteworthy that no signs of infection were observed in the biopsy sites in animals treated with Cp40. In fact, effective wound healing in the absence of C3 is supported by previous data showing somewhat accelerated healing in C3−/− mice when compared with the C3+/+ counterpart control. In the rodent model, increased numbers of basophils were present in the wounds of C3+/+ mice [43]. While no differential staining for inflammatory cells was performed in the cynomolgus monkey skin biopsies, increased numbers of granulocytes were detected in the blood of Cp40-treated animals, when compared with the control group.

Absence of infection in Cp40-treated animals is also supported by no apparent increase in the expression of inflammatory cytokines in tissues as well as healthy organs as noted by the histopathology. This supports the notion that lack of C3 resulting from a genetic dysfunction

may differ significantly from decreased levels of C3 as a consequence of therapeutic inhibition where minimal amounts of untargeted C3 may still be available to support opsonization and trigger immune responses. Further, it is likely that in the absence of systemic C3, C3 from myeloid and intracellular sources is sufficient to regulate immune functions [44, 45]. Indeed, here we have shown that the expression of C3 by the liver and spleen is unaffected by the Cp40 treatment. Also, the reported daily body production of 6 g of C3 [46] suggests that minimal amounts of uninhibited C3 may surround the organs, despite Cp40 treatment.

Transcriptional profiling of key proinflammatory cytokines in cynomolgus monkeys under C3 inhibition revealed that IL-22 was the only cytokine apparently affected by the Cp40 treatment. Increased expression of IL-22 was observed in the spleens of animals in the treatment group when compared with concurrent controls. While a connection between C3 and IL-22 has been previously reported in a mouse model of intestinal damage, where *C. difficile*-induced IL-22 upregulated the expression of C3 by the liver [47], this is the first evidence to our knowledge of IL-22 upregulation in response to Cp40-treatment. One may speculate that given the ability of IL-22 to promote tissue repair [48], it may be involved with the faster rate of healing in animals treated with Cp40 when compared with concurrent controls. Interestingly, tissue protection as a consequence of C3 inhibition was also observed in experimental sepsis in baboons [49, 50].

While our histopathology findings supported the absence of tissue damage or infectious or autoimmune disease in response to Cp40 treatment, they indicated local tissue irritation after multiple subcutaneous injections in the 3-month treatment study. The local irritation could potentially be circumvented by the use of subcutaneous pumps with slow infusion rate, decreasing the accumulation of compound at the site of injection. Further, new formulations of Cp40 analogs with increased solubility and improved pharmacokinetics are now available that may diminish local irritation via subcutaneous dosing [22]. Finally, plasma levels of C3 remained stable throughout the treatment period. This is an important observation in view of a previous study that had reported increased levels of C3 in response to the treatment with pegylated versions of the compound [34].

4. Conclusion

In summary, this is the first study reporting on the safety of systemic inhibition of C3 in non-human primates. Here we show data supporting the feasibility of complete inhibition of C3 for up to 3 months, without any adverse effects. These data offer fundamental information to guide further development of therapeutic agents that target complement proteins.

Supplementary Material

Refer to Web version on PubMed Central for supplementary material.

Acknowledgments

This study was supported by the US National Institutes of Health (#AI068730), the European Community's Seventh Framework Programme (602699 DIREKT), and the California National Primate Research Center base operating grant (#OD011107). We also thank Dr. Deborah McClellan for editorial assistance.

Financial disclosure

J.D.L. is the founder of Amyndas Pharmaceuticals, which is developing complement inhibitors (including third-generation compstatin analogues such as AMY-101) and inventor of patents or patent applications that describe the use of complement inhibitors for therapeutic purposes, some of which are developed by Amyndas Pharmaceuticals. J.D.L. is also the inventor of the compstatin technology licensed to Apellis Pharmaceuticals (4(1MeW)7W, also known as POT-4 and APL-1) and PEGylated derivatives such as APL-2. G.H. has a patent that describes the use of complement inhibitors for therapeutic purposes in periodontitis.

References

[1]. Hajishengallis G, Reis ES, Mastellos DC, Ricklin D, Lambris JD, Novel mechanisms and functions of complement, Nat Immunol, 18 (2017) 1288–1298. [PubMed: 29144501]

[2]. Merle NS, Church SE, Fremeaux-Bacchi V, Roumenina LT, Complement System Part I - Molecular Mechanisms of Activation and Regulation, Front Immunol, 6 (2015) 262. [PubMed: 26082779]

[3]. Ricklin D, Reis ES, Mastellos DC, Gros P, Lambris JD, Complement component C3 - The “Swiss Army Knife” of innate immunity and host defense, Immunol Rev, 274 (2016) 33–58. [PubMed: 27782325]

[4]. Ricklin D, Reis ES, Lambris JD, Complement in disease: a defence system turning offensive, Nat Rev Nephrol, 12 (2016) 383–401. [PubMed: 27211870]

[5]. Merle NS, Noe R, Halbwachs-Mecarelli L, Fremeaux-Bacchi V, Roumenina LT, Complement System Part II: Role in Immunity, Front Immunol, 6 (2015) 257. [PubMed: 26074922]

[6]. E SR, Falcao DA, Isaac L, Clinical aspects and molecular basis of primary deficiencies of complement component C3 and its regulatory proteins factor I and factor H, Scand J Immunol, 63 (2006) 155–168. [PubMed: 16499568]

[7]. de Cordoba SR, Tortajada A, Harris CL, Morgan BP, Complement dysregulation and disease: from genes and proteins to diagnostics and drugs, Immunobiology, 217 (2012) 1034–1046. [PubMed: 22964229]

[8]. Heurich M, Martinez-Barricarte R, Francis NJ, Roberts DL, Rodriguez de Cordoba S, Morgan BP, Harris CL, Common polymorphisms in C3, factor B, and factor H collaborate to determine systemic complement activity and disease risk, Proc Natl Acad Sci U S A, 108 (2011) 8761–8766. [PubMed: 21555552]

[9]. Risitano AM, Notaro R, Pascariello C, Sica M, del Vecchio L, Horvath CJ, Fridkis-Hareli M, Selleri C, Lindorfer MA, Taylor RP, Luzzatto L, Holers VM, The complement receptor 2/factor H fusion protein TT30 protects paroxysmal nocturnal hemoglobinuria erythrocytes from complement-mediated hemolysis and C3 fragment, Blood, 119 (2012) 6307–6316. [PubMed: 22577173]

[10]. Hakobyan S, Harding K, Aiyaz M, Hye A, Dobson R, Baird A, Liu B, Harris CL, Lovestone S, Morgan BP, Complement Biomarkers as Predictors of Disease Progression in Alzheimer’s Disease, J Alzheimers Dis, 54 (2016) 707–716. [PubMed: 27567854]

[11]. Jalal D, Renner B, Laskowski J, Stites E, Cooper J, Valente K, You Z, Perrenoud L,Le Quintrec M, Muhamed I, Christians U, Klawitter J, Lindorfer MA, Taylor RP, Holers VM, Thurman JM, Endothelial Microparticles and Systemic Complement Activation in Patients With Chronic Kidney Disease, J Am Heart Assoc, 7 (2018).

[12]. Bavia L, Lidani KCF, Andrade FA, Sobrinho M, Nisihara RM, de Messias-Reason IJ, Complement activation in acute myocardial infarction: An early marker of inflammation and tissue injury?, Immunol Lett, 200 (2018) 18–25. [PubMed: 29908956]

[13]. Doerner SK, Reis ES, Leung ES, Ko JS, Heaney JD, Berger NA, Lambris JD, Nadeau JH, High-Fat Diet-Induced Complement Activation Mediates Intestinal Inflammation and Neoplasia, Independent of Obesity, Mol Cancer Res, 14 (2016) 953–965. [PubMed: 27535705]

[14]. Krug N, Tschernig T, Erpenbeck VJ, Hohlfeld JM, Kohl J, Complement factors C3a and C5a are increased in bronchoalveolar lavage fluid after segmental allergen provocation in subjects with asthma, Am J Respir Crit Care Med, 164 (2001) 1841–1843. [PubMed: 11734433]

[15]. Reis ES, Mastellos DC, Ricklin D, Mantovani A, Lambris JD, Complement in cancer: untangling an intricate relationship, Nat Rev Immunol, 18 (2018) 5–18. [PubMed: 28920587]

[16]. Pratt JR, Basheer SA, Sacks SH, Local synthesis of complement component C3 regulates acute renal transplant rejection, Nat Med, 8 (2002) 582–587. [PubMed: 12042808]

[17]. Maekawa T, Briones RA, Resuello RR, Tuplano JV, Hajishengallis E, Kajikawa T, Koutsogiannaki S, Garcia CA, Ricklin D, Lambris JD, Hajishengallis G, Inhibition of pre-existing natural periodontitis in non-human primates by a locally administered peptide inhibitor of complement C3, J Clin Periodontol, 43 (2016) 238–249. [PubMed: 26728318]

[18]. Mastellos DC, Reis ES, Ricklin D, Smith RJ, Lambris JD, Complement C3-Targeted Therapy: Replacing Long-Held Assertions with Evidence-Based Discovery, Trends Immunol, 38 (2017) 383–394. [PubMed: 28416449]

[19]. Mastellos DC, Reis ES, Yancopoulou D, Hajishengallis G, Ricklin D, Lambris JD, From orphan drugs to adopted therapies: Advancing C3-targeted intervention to the clinical stage, Immunobiology, 221 (2016) 1046–1057. [PubMed: 27353192]

[20]. Ricklin D, Mastellos DC, Reis ES, Lambris JD, The renaissance of complement therapeutics, Nat Rev Nephrol, 14 (2018) 26–47. [PubMed: 29199277]

[21]. Mastellos DC, Yancopoulou D, Kokkinos P, Huber-Lang M, Hajishengallis G, Biglarnia AR, Lupu F, Nilsson B, Risitano AM, Ricklin D, Lambris JD, Compstatin: a C3-targeted complement inhibitor reaching its prime for bedside intervention, Eur J Clin Invest, 45 (2015) 423–440. [PubMed: 25678219]

[22]. Berger N, Alayi TD, Resuello RRG, Tuplano JV, Reis ES, Lambris JD, New Analogs of the Complement C3 Inhibitor Compstatin with Increased Solubility and Improved Pharmacokinetic Profile, J Med Chem, 61 (2018) 6153–6162. [PubMed: 29920096]

[23]. Reis ES, DeAngelis RA, Chen H, Resuello RR, Ricklin D, Lambris JD, Therapeutic C3 inhibitor Cp40 abrogates complement activation induced by modern hemodialysis filters, Immunobiology, 220 (2015) 476–482. [PubMed: 25468722]

[24]. Qu H, Ricklin D, Bai H, Chen H, Reis ES, Maciejewski M, Tzekou A, DeAngelis RA, Resuello RR, Lupu F, Barlow PN, Lambris JD, New analogs of the clinical complement inhibitor compstatin with subnanomolar affinity and enhanced pharmacokinetic properties, Immunobiology, 218 (2013) 496–505. [PubMed: 22795972]

[25]. Xie L, Xu F, Liu S, Ji Y, Zhou Q, Wu Q, Gong W, Cheng K, Li J, Li L, Fang L, Zhou L, Xie P, Age- and sex-based hematological and biochemical parameters for Macaca fascicularis, PLoS One, 8 (2013) e64892. [PubMed: 23762263]

[26]. Primikyri A, Papanastasiou M, Sarigiannis Y, Koutsogiannaki S, Reis ES, Tuplano JV, Resuello RR, Nilsson B, Ricklin D, Lambris JD, Method development and validation for the quantitation of the complement inhibitor Cp40 in human and cynomolgus monkey plasma by UPLC-ESI-MS, J Chromatogr B Analyt Technol Biomed Life Sci, 1041–1042 (2017) 19–26.

[27]. Alper CA, Johnson AM, Birtch AG, Moore FD, Human C'3: evidence for the liver as the primary site of synthesis, Science, 163 (1969) 286–288. [PubMed: 4883617]

[28]. Cavalieri RR, Iodine metabolism and thyroid physiology: current concepts, Thyroid, 7 (1997) 177–181. [PubMed: 9133680]

[29]. Norby EH, Neutze J, Van Nostrand D, Burman KD, Warren RW, Nasal radioiodine activity: a prospective study of frequency, intensity, and pattern, J Nucl Med, 31 (1990) 52–54. [PubMed: 2295940]

[30]. Larouche J, Sheoran S, Maruyama K, Martino MM, Immune Regulation of Skin Wound Healing: Mechanisms and Novel Therapeutic Targets, Adv Wound Care (New Rochelle), 7 (2018) 209–231. [PubMed: 29984112]

[31]. Barnum SR, Therapeutic Inhibition of Complement: Well Worth the Risk, Trends Pharmacol Sci, 38 (2017) 503–505. [PubMed: 28413098]

[32]. Morgan BP, Harris CL, Complement, a target for therapy in inflammatory and degenerative diseases, Nat Rev Drug Discov, 14 (2015) 857–877. [PubMed: 26493766]

[33]. Sicre de Fontbrune F, Peffault de Latour R, Ten Years of Clinical Experience With Eculizumab in Patients With Paroxysmal Nocturnal Hemoglobinuria, Semin Hematol, 55 (2018) 124–129. [PubMed: 30032748]

[34]. Cofiell R, Kukreja A, Bedard K, Yan Y, Mickle AP, Ogawa M, Bedrosian CL, Faas SJ, Eculizumab reduces complement activation, inflammation, endothelial damage, thrombosis, and renal injury markers in aHUS, Blood, 125 (2015) 3253–3262. [PubMed: 25833956]

[35]. Mastellos DC, Reis ES, Yancopoulou D, Risitano AM, Lambris JD, Expanding Complement Therapeutics for the Treatment of Paroxysmal Nocturnal Hemoglobinuria, Semin Hematol, 55 (2018) 167–175. [PubMed: 30032754]

[36]. Risitano AM, Ricklin D, Huang Y, Reis ES, Chen H, Ricci P, Lin Z, Pascariello C, Raia M, Sica M, Del Vecchio L, Pane F, Lupu F, Notaro R, Resuello RR, DeAngelis RA, Lambris JD, Peptide inhibitors of C3 activation as a novel strategy of complement inhibition for the treatment of paroxysmal nocturnal hemoglobinuria, Blood, 123 (2014) 2094–2101. [PubMed: 24497537]

[37]. van Griensven M, Ricklin D, Denk S, Halbgebauer R, Braun CK, Schultze A, Hones F, Koutsogiannaki S, Primikyri A, Reis E, Messerer D, Hafner S, Radermacher P, Biglarnia AR, Resuello RRG, Tuplano JV, Mayer B, Nilsson K, Nilsson B, Lambris JD, Huber-Lang M, Protective Effects of the Complement Inhibitor Compstatin CP40 in Hemorrhagic Shock, Shock, (2018).

[38]. Morita Y, Ikeguchi H, Nakamura J, Hotta N, Yuzawa Y, Matsuo S, Complement activation products in the urine from proteinuric patients, J Am Soc Nephrol, 11 (2000) 700–707. [PubMed: 10752529]

[39]. Sauter RJ, Sauter M, Reis ES, Emschermann FN, Nording H, Ebenhoch S, Kraft P, Munzer P, Mauler M, Rheinlaender J, Madlung J, Edlich F, Schaffer TE, Meuth SG, Duerschmied D, Geisler T, Borst O, Gawaz M, Kleinschnitz C, Lambris JD, Langer HF, A Functional Relevance of the Anaphylatoxin Receptor C3aR for Platelet Function and Arterial Thrombus Formation Marks an Intersection Point Between Innate Immunity and Thrombosis, Circulation, (2018).

[40]. Chen X, Arumugam TV, Cheng YL, Lee JH, Chigurupati S, Mattson MP, Basta M, Combination Therapy with Low-Dose IVIG and a C1-esterase Inhibitor Ameliorates Brain Damage and Functional Deficits in Experimental Ischemic Stroke, Neuromolecular Med, 20 (2018) 63–72. [PubMed: 29299869]

[41]. Radke A, Mottaghy K, Goldmann C, Khorram-Sefat R, Kovacs B, Janssen A, Klosterhalfen B, Hafemann B, Pallua N, Kirschfink M, C1 inhibitor prevents capillary leakage after thermal trauma, Crit Care Med, 28 (2000) 3224–3232. [PubMed: 11008986]

[42]. Bossi F, Tripodo C, Rizzi L, Bulla R, Agostinis C, Guarnotta C, Munaut C, Baldassarre G, Papa G, Zorzet S, Ghebrehiwet B, Ling GS, Botto M, Tedesco F, C1q as a unique player in angiogenesis with therapeutic implication in wound healing, Proc Natl Acad Sci U S A, 111 (2014) 4209–4214. [PubMed: 24591625]

[43]. Rafail S, Kourtzelis I, Foukas PG, Markiewski MM, DeAngelis RA, Guariento M, Ricklin D, Grice EA, Lambris JD, Complement deficiency promotes cutaneous wound healing in mice, J Immunol, 194 (2015) 1285–1291. [PubMed: 25548229]

[44]. Naughton MA, Botto M, Carter MJ, Alexander GJ, Goldman JM, Walport MJ, Extrahepatic secreted complement C3 contributes to circulating C3 levels in humans, J Immunol, 156 (1996) 3051–3056. [PubMed: 8609428]

[45]. Verschoor A, Brockman MA, Knipe DM, Carroll MC, Cutting edge: myeloid complement C3 enhances the humoral response to peripheral viral infection, J Immunol, 167 (2001) 2446–2451. [PubMed: 11509581]

[46]. Lachmann PJ, Smith RA, Taking complement to the clinic--has the time finally come?, Scand J Immunol, 69 (2009) 471–478. [PubMed: 19439007]

[47]. Hasegawa M, Yada S, Liu MZ, Kamada N, Munoz-Planillo R, Do N, Nunez G, Inohara N, Interleukin-22 regulates the complement system to promote resistance against pathobionts after pathogen-induced intestinal damage, Immunity, 41 (2014) 620–632. [PubMed: 25367575]

[48]. McGee HM, Schmidt BA, Booth CJ, Yancopoulos GD, Valenzuela DM, Murphy AJ, Stevens S, Flavell RA, Horsley V, IL-22 promotes fibroblast-mediated wound repair in the skin, J Invest Dermatol, 133 (2013) 1321–1329. [PubMed: 23223145]

[49]. Silasi-Mansat R, Zhu H, Georgescu C, Popescu N, Keshari RS, Peer G, Lupu C, Taylor FB, Pereira HA, Kinasewitz G, Lambris JD, Lupu F, Complement inhibition decreases early fibrogenic events in the lung of septic baboons, J Cell Mol Med, 19 (2015) 2549–2563. [PubMed: 26337158]

[50]. Silasi-Mansat R, Zhu H, Popescu NI, Peer G, Sfyroera G, Magotti P, Ivanciu L, Lupu C, Mollnes TE, Taylor FB, Kinasewitz G, Lambris JD, Lupu F, Complement inhibition decreases the procoagulant response and confers organ protection in a baboon model of Escherichia coli sepsis, Blood, 116 (2010) 1002–1010. [PubMed: 20466856]

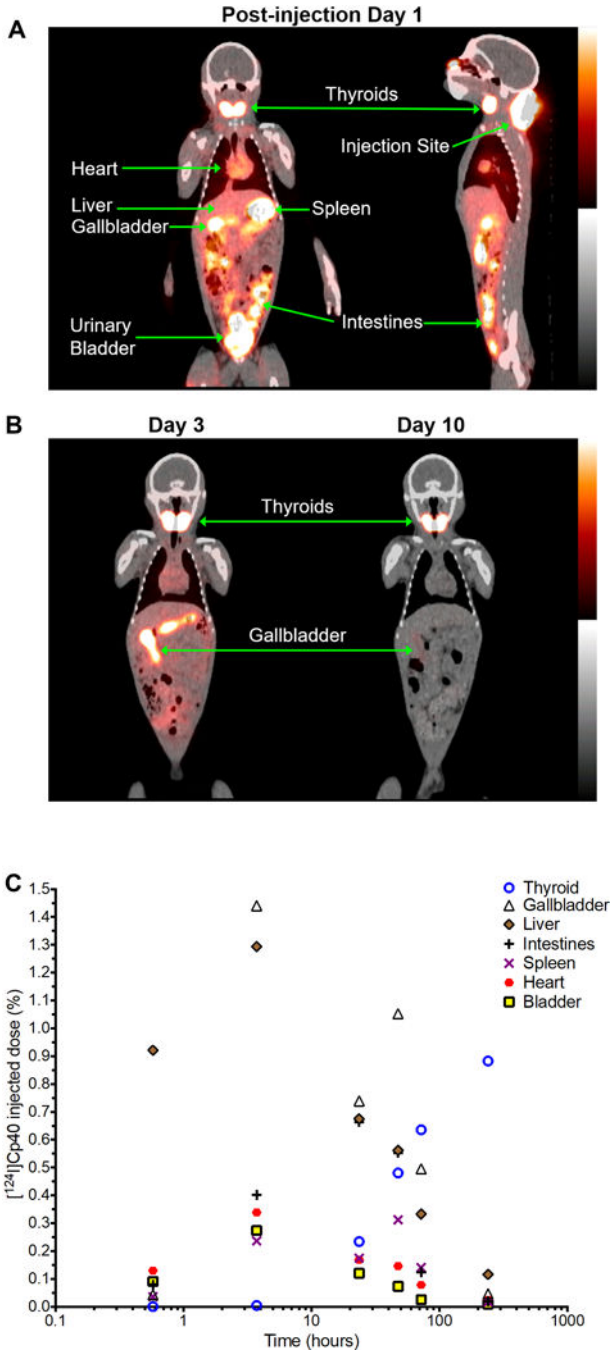

Figure 1. ***In vivo*** **biodistribution of [^{124}I]Cp40 is associated with the presence of C3.**

A. Coronal and sagittal fused PET/CT images of female rhesus monkey acquired 1 day after a single injection of [^{124}I]Cp40. **B.** Coronal fused PET/CT images of same animal acquired 3 and 10 days after the same injection of [^{124}I]Cp40. The same PET (0 to 7 kBq) and CT (−160 to 240 HU) scales were used for all images. **C.** Regional percentages of injected [^{124}I]Cp40. The [^{124}I]Cp40 subcutaneous injection site retained a pool of [^{124}I]Cp40 dose that steadily decreased in percentage of injected dose corresponding to the aforementioned

post-injection times: 64%, 54%, 45%, 40%, 37%, and 19% (data not plotted above). Thyroid uptake of [^{124}I]Cp40 continuously increased over the 10-day period.

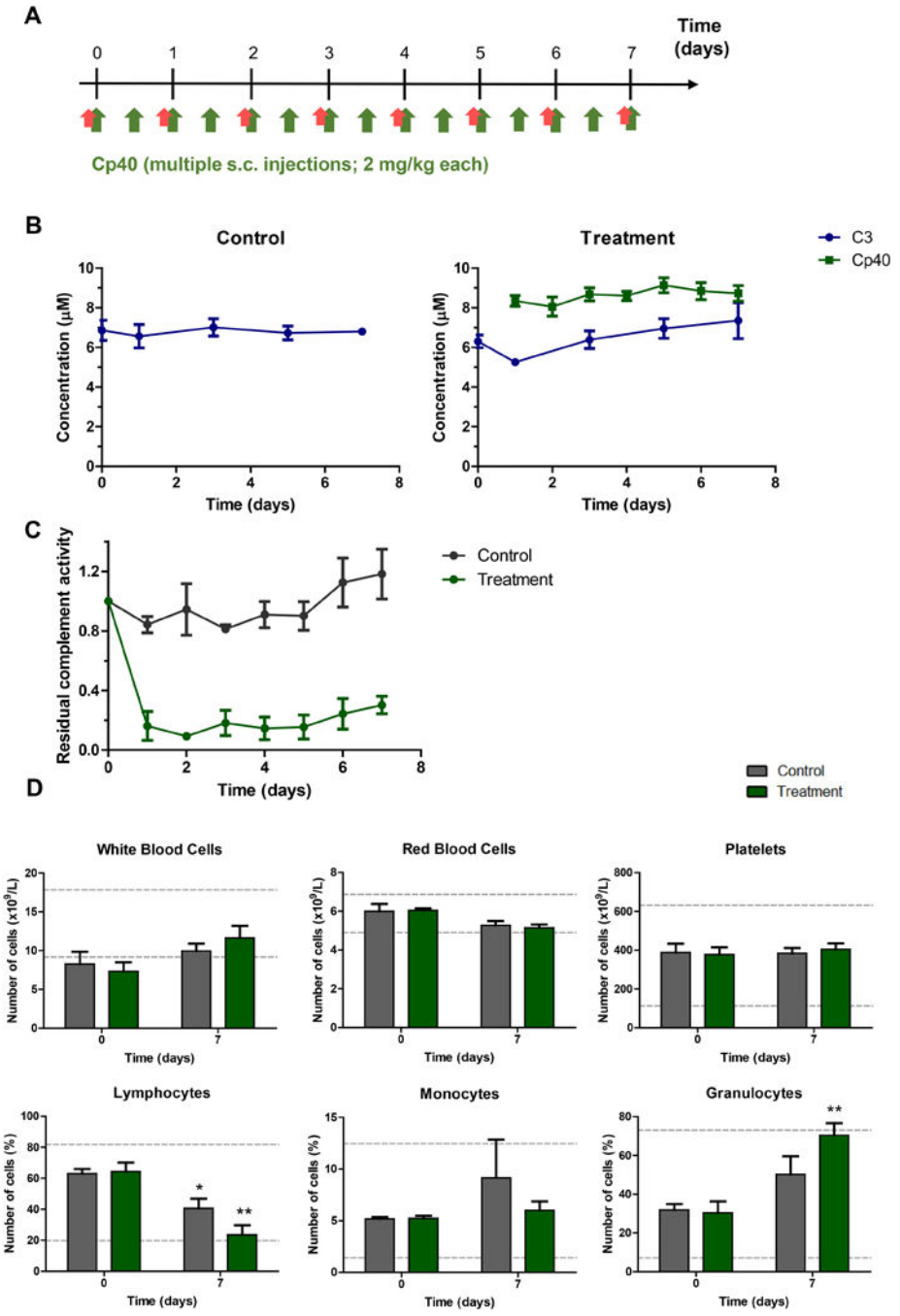

Figure 2. ***In vivo*** **C3 inhibition during a one-week period.**

A. Schematics showing Cp40 dosing (green arrows) and blood collection points (red arrows). Cp40 was injected subcutaneously (s.c.) into four male cynomolgus monkeys at a dose of 2 mg/kg every 12 h (a total of 15 injections). In parallel, vehicle alone was injected into four control male monkeys following the same injection scheme. Blood samples were collected every 24 h for a total of 7 days. **B.** Plasma concentrations of Cp40 and C3 were determined by ultra-performance liquid chromatography-high definition mass spectrometry and nephelometry, respectively. **C.** Residual activation of the complement alternative

pathway was measured over time in the plasma samples of cynomolgus monkeys treated with Cp40 and vehicle-injected control. The graph depicts relative values in relation to activation detected in time point day 0 (before the first injection), defined as 100% activation. **D.** Hematological parameters were measured in the plasma samples of cynomolgus monkeys treated with Cp40 or vehicle on days 0 and 7. The dotted lines depict the range of normal values previously determined in cynomolgus monkeys [25]. Data are shown as means ± S.E.M. (n=4/ group).

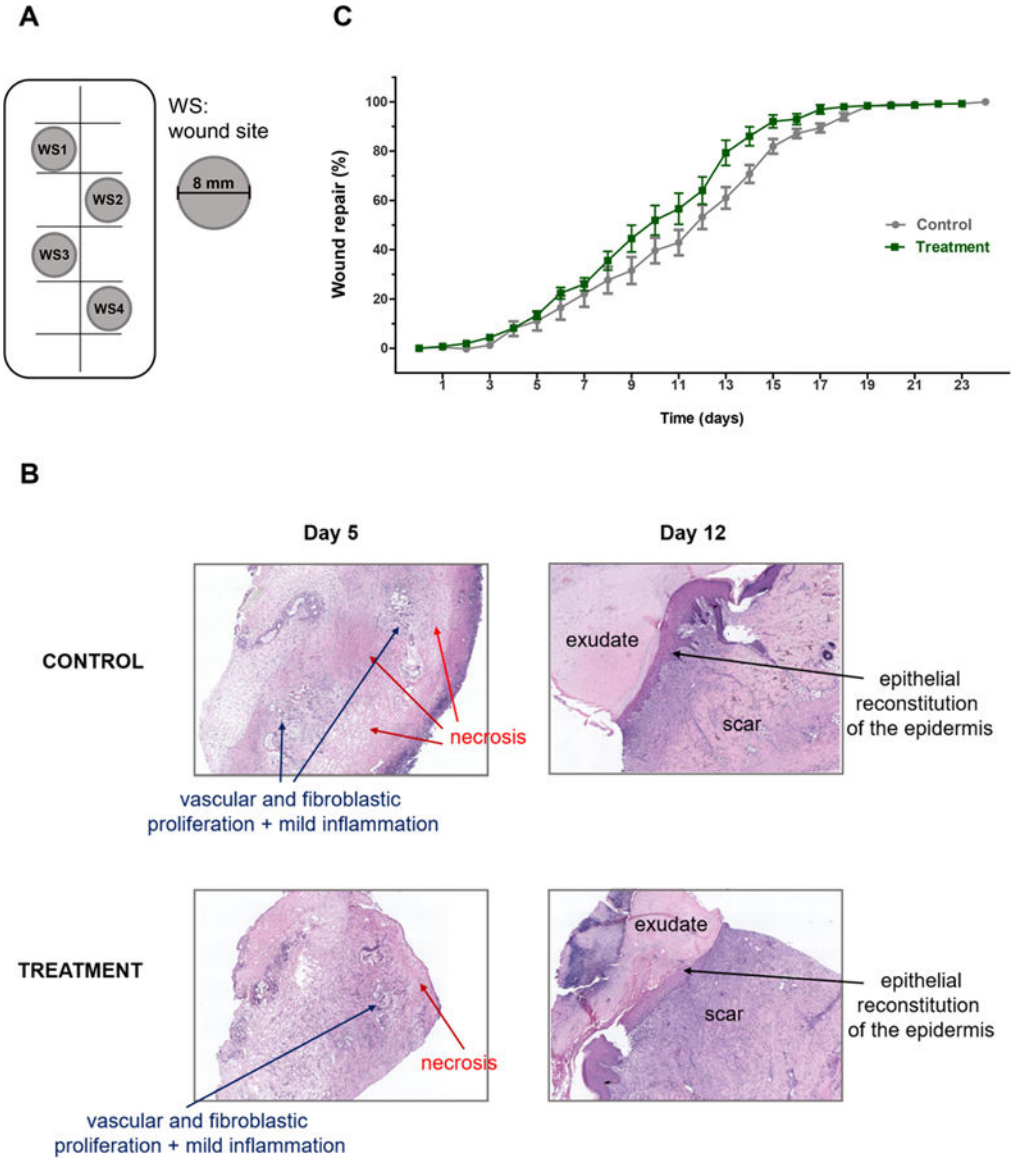

Figure 3. C3 inhibition assists healing of cutaneous wounds.

A total of four punch biopsies (8-mm diameter each) were taken from the dorsal side of cynomolgus monkeys 3 h after an initial subcutaneous injection of Cp40 or vehicle. Cp40 treatment was conducted for a week as indicated in Figure 1. **A.** Schematics showing distribution of wound sites on the dorsal side of the monkeys. **B.** Histological analysis of H&E-stained skin on days 5 and 12 post-biopsy, from animals in the control and Cp40-treatment groups. The figure shows representative scanned slides (2× magnification). **C.** The borders of the wounds were marked using indelible, nontoxic ink, and the size of each site was monitored daily until complete healing was observed. Sites were digitally photographed, and ImageJ software was used to calculate changes in wound area over time. Healing of the biopsy sites were calculated as percentage of the original wound area. Data are shown as means ± S.E.M. (n=4/ group).

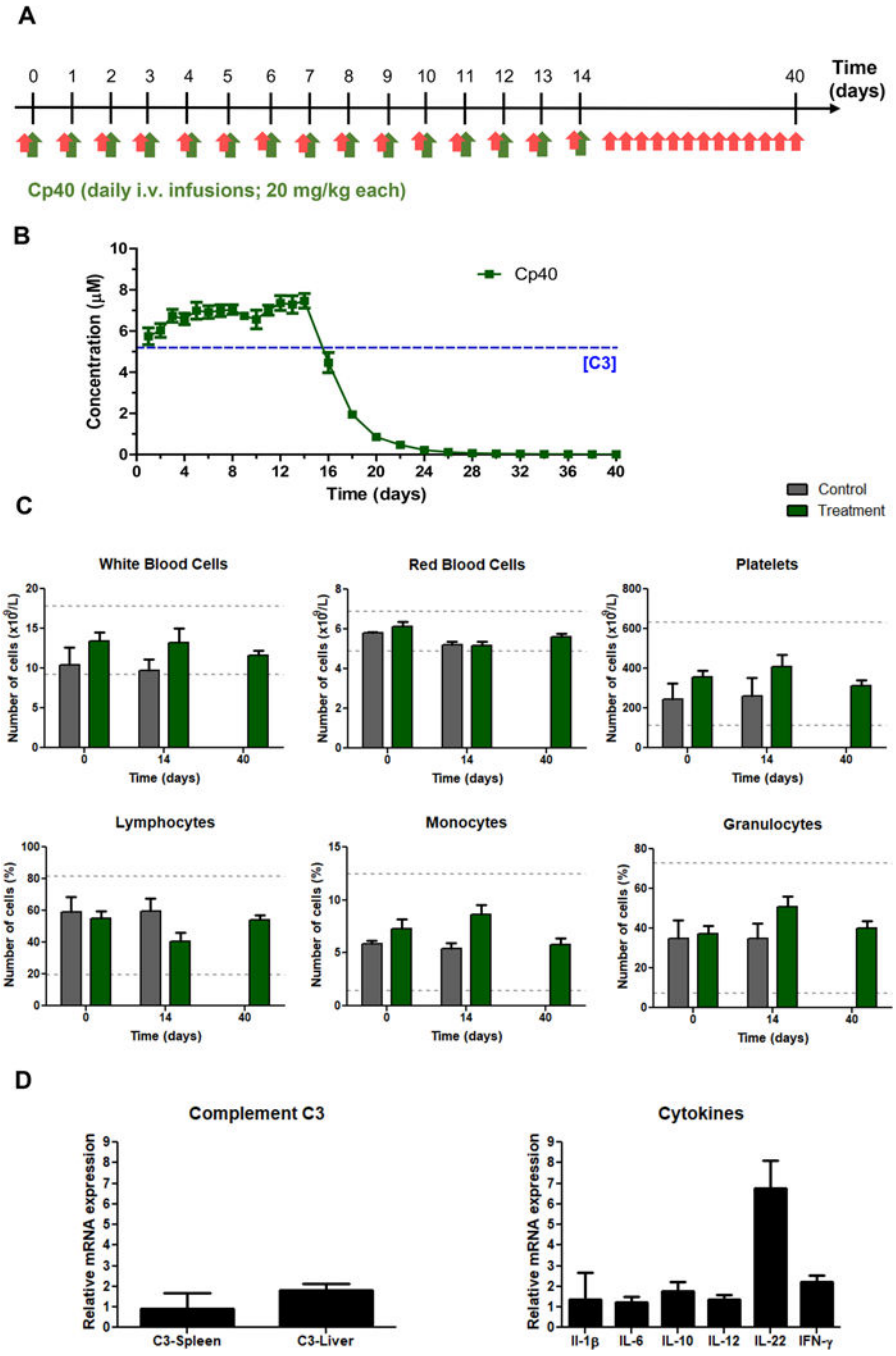

Figure 4. ***In vivo*** **C3 inhibition during a two-week period.**

A. Schematics showing Cp40 dosing (green arrows) and blood collection points (red arrows). Cp40 was infused intravenously each day into six male cynomolgus monkeys at a dose of 20 mg/kg (a total of 15 injections). In parallel, vehicle alone was infused into three control male monkeys following the same injection scheme. Blood samples were collected every 24 h for a total of 14 days, followed by collections every 48 h on days 14–40. **B.** Plasma concentrations of Cp40 was determined by ultra-performance liquid chromatography-high definition mass spectrometry. The blue dotted line depicts the mean

C3 concentration observed in cynomolgus monkeys. **C.** Hematological parameters were measured in the plasma samples of monkeys treated with Cp40 or vehicle on days 0, 14, and 40. The dotted lines depict the range of normal values previously determined in cynomolgus monkeys [25]. **D.** Spleen and liver tissues were collected on day 40. Relative mRNA expression of C3 and cytokines was determined by quantitative real-time PCR. The graphs depict the relative amounts of gene expression in tissues from monkeys in the treatment group in relation to the control group. Data are shown as means ± S.E.M. (Control group: n=3; Treatment group: n=6).

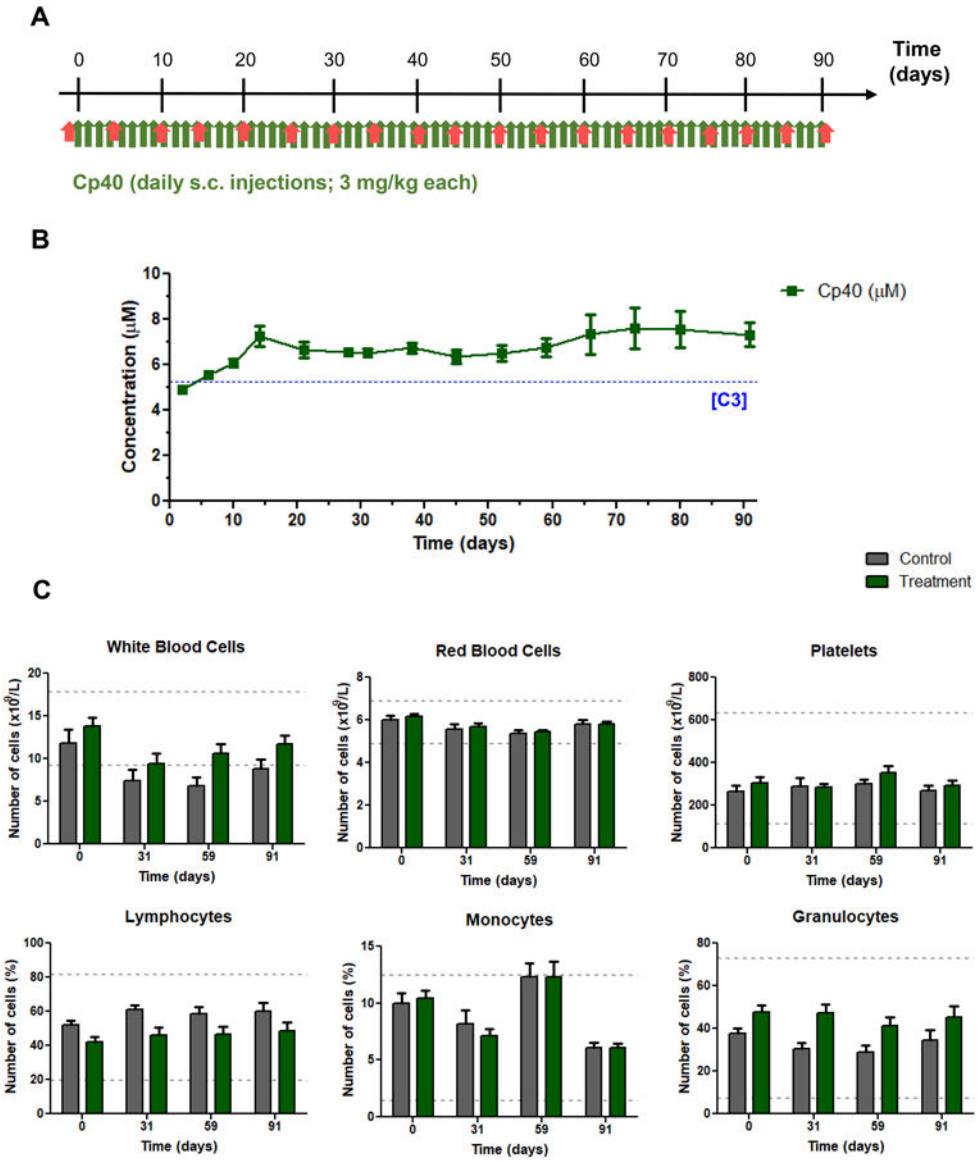

Figure 5. ***In vivo*** **C3 inhibition during a three-month period.**

A. Schematics showing Cp40 dosing (green arrows) and blood collection points (red arrows). Cp40 was injected subcutaneously (s.c.) daily into four male and four female cynomolgus monkeys at a dose of 3 mg/kg (a total of 91 injections). In parallel, vehicle alone was injected s.c. into four male and four female control monkeys following the same injection scheme. Blood samples were collected weekly or bi-weekly during the three-month period. **B.** Plasma concentrations of Cp40 were determined by ultra-performance liquid chromatography-high definition mass spectrometry. The blue dotted line depicts the mean C3 concentration observed in cynomolgus monkeys. **C.** Hematological parameters were measured in the plasma samples of monkeys treated with Cp40 or vehicle on days 0, 31, 59, and 91. The dotted lines depict the range of normal values previously determined in cynomolgus monkeys [25]. Data are shown as means ± S.E.M. (n=8/group).